HAMON, C., MARCHAND, R., LAURENT, Y. & LANG, J. (1974). *Bull. Soc. Fr. Minér. Crist.* **97**, 6–12.

HUGHES, E. W. (1941). *J. Amer. Chem. Soc.* **63**, 1737.

International Tables for X-ray Crystallography (1952). Vol. I. Birmingham: Kynoch Press.

KEVE, E. T. & SKAPSKI, A. C. (1968). *Inorg. Chem.* **2**, 1757–1761.

LAURENT, Y., LANG, J. & LE BIHAN, M. T. (1968). *Acta Cryst.* **B24**, 494–499.

LAURENT, Y., LANG, J. & LE BIHAN, M. T. (1969). *Acta Cryst.* **B25**, 199–203.

MARTINEZ-RIPOLL, M., HAASE, A. & BRAUER, G. (1973). *Acta Cryst.* **B29**, 1715–1717.

MOORE, F. H. (1963). *Acta Cryst.* **16**, 1169–1175.

PREWITT, C. T. (1962). Oak Ridge National Laboratory Report ORNL-TM-305.

VAND, V., EILAND, P. F. & PEPINSKY, R. (1957). *Acta Cryst.* **10**, 303–306.

A Liquid-Nitrogen Temperature Study of the Pyrene-d8-Tetracyanoethylene Charge-Transfer Complex

BY F. KREBS LARSEN,* R. G. LITTLE† AND P. COPPENS

Department of Chemistry, State University of New York at Buffalo, Buffalo, New York 14214, *U.S.A.*

A liquid-nitrogen temperature diffraction analysis of the charge-transfer complex pyrene-d8-tetracyanoethylene is described. The cell dimensions at 105 K are $a = 14\cdot136$ (5), $b = 7\cdot169$ (2), $c = 7\cdot866$ (2) Å, $\beta = 91\cdot73$ (2)°. Although the data refine easily to $R(F) = 5\cdot1\%$ and $R_w(F) = 3\cdot8\%$, difference maps indicate disorder in the plane of the tetracyanoethylene molecule. Subsequent refinement with two superimposed TCNE molecules, whose geometries were constrained to be equal and whose thermal motion was restricted to rigid-body motion, converged at $R(F) = 4\cdot7\%$ and $R_w(F) = 3\cdot6\%$, showing an arrangement of TCNE molecules in two orientations with a relative rotation of 90° around the center of the molecule in the molecular plane. 7% of the molecules are in the alternative orientation which corresponds to an energy difference of at least 0·54 kcal mole^{-1}. Comparison of the geometries of the component molecules with those in the non-complexed crystals indicates effects of complexing on bond lengths to be at, or smaller than, the limit of the experimental accuracy. Integration of the charge density over the volume of the TCNE molecule shows the transfer of charge between the molecules in the crystal to be very small ($< 0\cdot15e$). This conclusion is confirmed by a refinement of the occupancy of the spherical valence shells of the constituent atoms.

Introduction

Charge-transfer complexes between tetracyanoethylene (TCNE) and aromatic hydrocarbons have been the subject of many experimental studies. The general feature that the TCNE and the hydrocarbon molecules are alternately stacked with parallel molecular planes is well established in several complexes: naphthalene–TCNE (Williams & Wallwork, 1967); ferrocene–TCNE (Adman, Rosenblum, Sullivan & Margulis, 1967); pyrene–TCNE (Ikemoto & Kuroda, 1968); perylene–TCNE (Ikemoto, Yakushi & Kuroda, 1970); paracyclophane–TCNE (Bernstein & Trueblood, 1971).

The effect of complexing on the geometry of the constituents is smaller than the experimental accuracy achieved in most of these studies. However, a better accuracy can be obtained with present diffractometer and data-processing techniques and accurate studies on

crystals of the pure compounds and their complexes could lead to improved understanding of the interactions between the molecules. Recently results of precise studies of molecular pyrene by X-ray diffraction (Allmann, 1970) and neutron diffraction (Hazell, Larsen & Lehmann, 1972) became available. The molecular geometry of TCNE is also well known for the pure compound. A monoclinic modification was described by Bekoe & Trueblood (1960, 1964). The cubic modification has been studied with X-rays by Coulter (1960) and Little, Pautler & Coppens (1971), and with neutrons by Becker, Coppens & Ross (1973), while Hope (1968) performed an electron diffraction analysis of the molecule in the gas phase. Here we report a low-temperature study of pyrene-d8–TCNE and a comparison of the molecular geometry in the charge-transfer complexed state with the geometry of the individual molecules in the non-complexed state.

The nature of the bonding and the electron distribution in charge-transfer complexes have been the subject of a great many studies [for a survey see Foster (1969), chap. 2]. A second aim of the present study was to test the accepted theoretical concepts against the in-

---

* Present address: Department of Chemistry, University of Aarhus, DK-8000 Aarhus C, Denmark.

† Present address: Department of Chemistry and Materials Research Center, Northwestern University, Evanston, Illinois 60201, U.S.A.

formation on molecular charge distributions that can be extracted from accurate diffraction data.

Experimental

X-ray intensity data were collected at 105 K on a Picker diffractometer. Cooling was achieved by blowing a cold N_2 gas stream over the crystal. The cooling equipment was an extensively modified MRC (Materials Research Corporation) cryocollimator. N_2 gas is obtained by evaporation of the liquid and passed through a phase separator into a cooling spiral submerged in the liquid N_2. The cold gas escapes through a flexible transfer line, which is aimed at the crystal; as was realized later, this method has the disadvantage that there is no pressure regulation between the surface of liquid N_2 in the Dewar and the outlet through the nozzle.*

In order to prevent frost formation on the crystal the cold gas stream was surrounded by a stream of warm, dry N_2 gas from another source. In addition we found it necessary to surround the entire diffractometer by a dry box. The temperature of the cold gas can be regulated by a heating wire in the flexible transfer line. A thermocouple in the nozzle near the crystal was connected to a temperature controller which kept the temperature at the thermocouple constant within ± 1 K. However, the intensity of a high-order standard reflection – 617 at $\sin \theta/\lambda = 0.5$ $\mathring{A}^{-1}$ – oscillated in a manner indicating temperature fluctuations of up to 6 K during nitrogen refill of the intermediate Dewar.

These fluctuations are attributed to a change in the relative velocity of the inner and outer streams, which, because of turbulence, may cause a change in temperature, even though the inner-stream temperature in the nozzle is kept constant by a temperature controller. To eliminate any effect on the intensity data set, the instrument was wired to print a signal during nitrogen refill, and reflections measured during this instability were later remeasured under standard conditions.

The best overall temperature stability was achieved at high flow rates. Average consumption of liquid nitrogen under these conditions was 9 litre h^{-1}.

The crystal data for perdeuteropyrene–TCNE at 105 K and the room-temperature data for the hydrogenated compound are listed in Table 1. The unit-cell parameters for the low-temperature study were determined on the Picker diffractometer using graphite-monochromatized Mo $K\alpha$ radiation. 20 high-order reflections (14 with $2\theta > 60°$) were carefully centered for Mo $K\alpha_1$ radiation, $\lambda = 0.7092$ $\mathring{A}$, on both positive and negative sides of the 2θ circle using a narrow receiving aperture. The $K\alpha_1$ and $K\alpha_2$ peaks were clearly resolved. The lattice constants were obtained from a least-

* The data for this study were collected in 1969. Presently our low-temperature data are collected with a cryostat which eliminates many of the problems described here (Coppens et al., 1974).

squares refinement (Busing & Levy, 1967) of the observed angle settings.

Table 1. *Crystal data for perdeuteropyrene–TCNE* $(C_{16}D_{10}.C_6N_4)$ *at* 105 K *and* $C_{16}H_{10}.C_6N_6$ *at room temperature*

Space group	105°K $P2_1/a$	Room temperature* $P2_1/a$
a	14·136 (5) $\mathring{A}$	14·333 (9) $\mathring{A}$
b	7·169 (2)	7·242 (8)
c	7·866 (2)	7·978 (4)
β	91·73 (2)°	92·36 (4)°
Z	2	2
V	796·75 $\mathring{A}^3$	827·5 $\mathring{A}^3$
μ	0·846 cm^{-1}	7·5 cm^{-1} (Cu $K\alpha$)

* Ikemoto & Kuroda (1968).

The crystal used for data collection was grown by slow evaporation of a solution of perdeuteropyrene and TCNE dissolved in ethyl acetate. Its linear dimensions are about $0.2 \times 0.2 \times 0.4$ mm. The crystal was mounted in a capillary to prevent sublimation.

The intensity measurement of each reflection was performed by a θ–2θ continuous scan. The scan range, $R(\theta)$ was varied according to the dispersion relation, $R(\theta) = R(\theta = 0) + 0.692 \tan \theta$ for Mo radiation. The basic scan range used was $2.9°$, and the scan rate was $1°$ min^{-1}.

Stationary-counter background counts of 10 s were taken at each end of the scan range. The source collimator had a diameter of 1 mm and the receiving aperture was a collimator of 2 mm diameter positioned in front of the scintillation counter with the opening 3.5 cm from the crystal. A number of reflections had peak count rates in excess of the linear response of the counting chain. Those reflections and approximately 50 additional reflections of medium intensity were re-collected at a reduced tube voltage. A scale factor between the two sets was calculated from the 50 reflections common to both. Three standard reflections were measured every 30 measurements, which was approximately every two hours. Two of these are intense, low-order reflections (400 and 020). The third is the fairly intense 617 reflection at $\sin \theta/\lambda = 0.5$ $\mathring{A}^{-1}$ which was selected to monitor the temperature changes previously mentioned. No general trend in the intensities of the two low-order standard reflections was observed. 5476 reflections were collected, that is one full set with $2\theta < 75°$, $\sin \theta/\lambda < 0.87$ $\mathring{A}^{-1}$, plus some symmetry-related reflections, well distributed in reciprocal space. The standard reflections with weights based on statistical accuracy were used to eliminate intensity fluctuations. Standard deviations were related to the intensities according to the formula: $\sigma^2(I) = \sigma^2(\text{stat}) + c^2(I)^2$, with $c = 0.015$, in which I is the background-corrected intensity of the reflection and $\sigma^2(\text{stat})$ is the contribution due to counting statistics.

The values of I and $\sigma(I)$ were corrected for Lorentz–polarization and absorption effects, though the trans-

mission factor varied only between 0·984 and 0·988. Values of F^2 for each equivalent set of reflections were averaged to yield 4040 reflections. 1844 of the intensities were greater than 3 standard deviations.

Least-squares refinement

The results from an earlier room-temperature study (Ikemoto & Kuroda, 1968) were used as initial parameters in the full-matrix least-squares refinement. Reflections for which $F^2 < 3\sigma(F^2)$ were only included in the refinement when $F^2_{calc} > 3\sigma(F^2)$, in which case F^2_{obs} was set equal to $3\sigma(F^2)$. Scale and isotropic extinction factors, positional and anisotropic temperature fac-

tors (except for hydrogen atoms) were refined in a full-matrix least-squares procedure based on F^2. The refinement converged at $R = \sum|F_o - k|F_c||/\sum F_o = 5·1\%$ and $R_w = \{(\sum w|F_o - k^2|F_c||^2)/\sum wF_o^2\}^{1/2} = 3·8\%$; the corresponding values based on F^2 are $R(F^2) = 6·3\%$, and $R_w(F^2) = 7·5\%$. Final positional parameters and temperature factors from this refinement are listed in Table 2 and Table 3 respectively.

Difference maps through the plane of the pyrene molecule (Fig. 1a) and the plane of the tetracyano-

Table 2. *Atomic coordinates expressed as fractions of the cell edges*

Top row for each atom corresponds to ordered model, bottom row to disordered model (2). For the ordered model the estimated standard deviation in units of least significant digit is given in parentheses; e. s. d.'s for the disordered model are very similar to those for the ordered model and not given explicitly. Primed letters denote the coordinates of the less populated TCNE molecular position for which the standard deviations are about 10 times those of the most populated TCNE molecular position.

|	x/a	y/b	z/c
C(1)	0·14502 (13)	−0·27599 (29)	0·26852 (23)
	0·14502	−0·27624	0·26860
C(2)	0·17603 (13)	−0·10128 (27)	0·21807 (22)
	0·17612	−0·10105	0·21825
C(3)	0·11991 (12)	0·01085 (25)	0·10956 (21)
	0·11986	0·01089	0·10949
C(4)	0·02928 (12)	−0·05608 (24)	0·05493 (21)
	0·02923	−0·05571	0·05482
C(5)	−0·00227 (12)	−0·23351 (25)	0·10901 (21)
	−0·00226	−0·23363	0·10918
C(6)	0·05667 (13)	−0·34171 (28)	0·21573 (22)
	0·05628	−0·34165	0·21566
C(7)	0·15000 (12)	0·19128 (27)	0·05264 (21)
	0·15012	0·19131	0·05276
C(8)	0·09452 (12)	0·29671 (26)	−0·05171 (22)
	0·09455	0·29670	−0·05176
D(1)	0·1822 (13)	−0·3534 (31)	0·3453 (24)
	0·1853	−0·3532	0·3493
D(2)	0·2332 (14)	−0·0558 (25)	0·2571 (23)
	0·2325	−0·0584	0·2566
D(6)	0·0330 (13)	−0·4607 (28)	0·2463 (23)
	0·0338	−0·4637	0·2478
D(7)	0·2102 (13)	0·2375 (27)	0·0886 (22)
	0·2116	0·2355	0·0887
D(8)	0·1143 (13)	0·4220 (28)	−0·0937 (24)
	0·1130	0·4169	−0·0909
C(9)	0·04366 (13)	0·00975 (27)	0·53472 (23)
	0·04402	0·00964	0·53482
C(10)	0·08594 (12)	−0·13813 (27)	0·63766 (22)
	0·08672	−0·13645	0·63773
C(11)	0·09827 (12)	0·17794 (28)	0·50801 (22)
	0·09861	0·17705	0·50886
N(1)	0·12178 (12)	−0·24944 (24)	0·71924 (20)
	0·12095	−0·25147	0·71929
N(2)	0·14287 (11)	0·30806 (24)	0·48982 (21)
	0·14221	0·30912	0·48887
C'(9)	−0·0032	−0·0857	0·5352
C'(10)	−0·0874	−0·1980	0·5104
C'(11)	0·0737	−0·1627	0·6378
N'(1)	−0·1537	−0·2876	0·4913
N'(2)	0·1343	−0·2245	0·7192

(a)

(b)
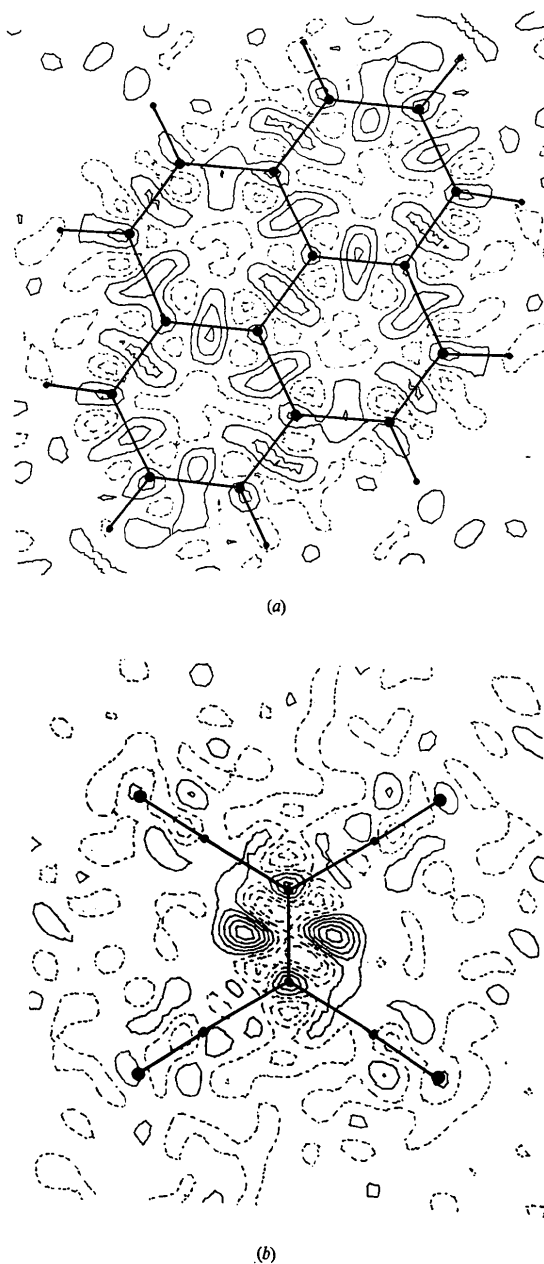
Fig. 1. Difference Fourier density in the plane of the TCNE (a) and the pyrene (b) molecules after ordered model refinement. Contour interval is 0·15 e Å⁻³; negative contours are broken.

Table 3. *Thermal parameters in* $\text{Å}^2 \times 10^4$

Estimated standard deviations in units of least significant digit are given in parentheses. Top row for each atom corresponds to the ordered model and the bottom row shows thermal parameters for the disordered model (2) as calculated from the T and L tensors found in the constrained refinement. Primed symbols denote the thermal parameters of the less populated TCNE molecular position. For the non-hydrogen atoms the temperature factor is of the form $\exp[-2\pi^2(\sum_i\sum_j h_i h_j a_i^* a_j^* U_{ij})]$.

	U_{11}	U_{22}	U_{33}	U_{12}	U_{13}	U_{23}
C(1)	229 (9)	235 (10)	169 (8)	65 (8)	13 (7)	28 (8)
	217	240	164	62	12	21
C(2)	168 (8)	250 (10)	156 (8)	24 (7)	2 (6)	−5 (7)
	165	256	157	25	1	−2
C(3)	155 (7)	186 (9)	151 (7)	4 (7)	21 (6)	−16 (7)
	148	189	139	−3	13	−13
C(4)	138 (7)	150 (8)	116 (7)	3 (6)	11 (5)	−10 (6)
	146	145	122	2	22	−12
C(5)	163 (8)	165 (9)	135 (6)	−1 (7)	15 (6)	−8 (7)
	185	148	145	0	27	0
C(6)	236 (9)	162 (9)	179 (8)	17 (7)	40 (7)	21 (7)
	238	176	169	32	29	22
C(7)	172 (8)	214 (7)	181 (8)	−48 (7)	15 (7)	−19 (7)
	173	209	180	−44	13	−14
C(8)	239 (9)	165 (9)	178 (8)	−45 (7)	41 (7)	−1 (7)
	208	169	185	−41	26	−2
D(1)	232 (53)					
	265	305	192	102	5	44
D(2)	144 (50)					
	168	333	186	18	−16	−3
D(6)	156 (51)					
	311	178	213	30	38	43
D(7)	178 (52)					
	191	276	227	−77	1	−15
D(8)	165 (51)					
	272	184	239	−68	32	12
C(9)	242 (8)	220 (9)	180 (8)	21 (8)	30 (6)	2 (8)
	184	203	150	20	−7	−7
C(10)	196 (8)	232 (10)	165 (8)	32 (7)	−13 (6)	−6 (7)
	198	217	152	35	−9	−6
C(11)	200 (8)	236 (9)	158 (8)	−2 (7)	−18 (6)	−19 (7)
	199	218	159	3	−3	−11
N(1)	267 (8)	288 (9)	218 (7)	72 (7)	−15 (6)	29 (7)
	241	251	217	43	−39	26
N(2)	274 (9)	275 (9)	245 (8)	−44 (7)	−2 (6)	−8 (8)
	245	253	234	37	−24	15
C′(9)	197	209	191	11	−25	14
C′(10)	213	225	203	−7	−23	12
C′(11)	212	224	196	25	−29	16
N′(1)	222	242	162	−20	8	−22
N′(2)	218	240	145	60	−7	−11

Table 4(*a*). *Summary of some results of various refinements on pyrene-d_8-TCNE*

Type of Refinement	Model characteristics	$R(F)$	$R_w(F)$	Number of variables	Number of reflections	Occupancy factor for TCNE2	Net charge (electrons) on one TCNE molecule
1. Conventional full-matrix least squares	Ordered model, unconstrained	5·1	3·8	139	1844	1·00	
2. Constrained least squares	TCNE disorder, two TCNE molecules constrained to be identical and of *mmm* symmetry $\varphi_{TCNE2} = \varphi_{TCNE1} + 90°$	4·7	3·6	73	1839	0·930 (3)	
3. —	As 2, all Euler angles refined independently	4·7	3·6	76	1841	0·930 (3)	
4. Extended L shell (ELS)	Ordered model unconstrained	4·7	3·3	157	1843	1·00	+0·21
5. —	Disordered model, TCNE2 positional and TCNE2 and deuterium thermal parameters from 2	4·2	2·9	152	1849	0·930	+0·07

Table 4(b). *Eulerian angles in radians, model 2*

	Perdeuteropyrene	TCNE major
φ	1·6382 (1)	2·3506 (6)
θ	0·6344 (1)	0·6140 (4)
ψ	−0·8713 (1)	−0·7919 (6)

ethylene molecule (Fig. 1b) show density in the bonding regions of the C–C bonds in pyrene and the single C–C and triple C≡N bonds in TCNE. An unexpected peak of 0·7 e Å⁻³ is observed, however, in the plane of the TCNE molecule on the normal to the central C=C bond. A similar feature in the charge-transfer complex paracyclophane–TCNE was explained by Bernstein & Trueblood (1971), by a disordered arrangement in which about 25% of the TCNE molecules are rotated by 90° around the center of the molecule in the molecular plane. As the molecule is approximately square, this rotation results in an approximate superposition of the cyano groups.

A similar model for perdeuteropyrene–TCNE was investigated with a least-squares program constructed to facilitate the refinement of constrained models (Pawley, 1971). The orientation of a molecular coordinate system is described by the Eulerian angles φ, θ, Ψ [for the definition of these angles and the reference coordinate system, see Pawley (1971)]. The molecular coordinate systems for the TCNE and pyrene molecules were defined so that the angle φ describes the rotation around the normal to the molecular plane. The anisotropic temperature factors are determined by three tensors, **T**, **L** and **S**, respectively the mean-square translational displacement, the mean-square librational displacement, and the screw rotation correlation (Schomaker & Trueblood, 1968). As both molecules occupy centers of symmetry the librational axes intersect and the **S** tensor is equal to zero.

A number of refinements of different constrained models were tested to elucidate the type and degree of disorder of the arrangement of the TCNE molecules. All included an isotropic extinction parameter as a variable. Results are listed in Table 4. In the most successful model (2), the pyrene and TCNE molecules are considered rigid and the TCNE molecules are constrained to *mmm* symmetry. A fraction of the TCNE molecules – expressed as an occupancy factor – is
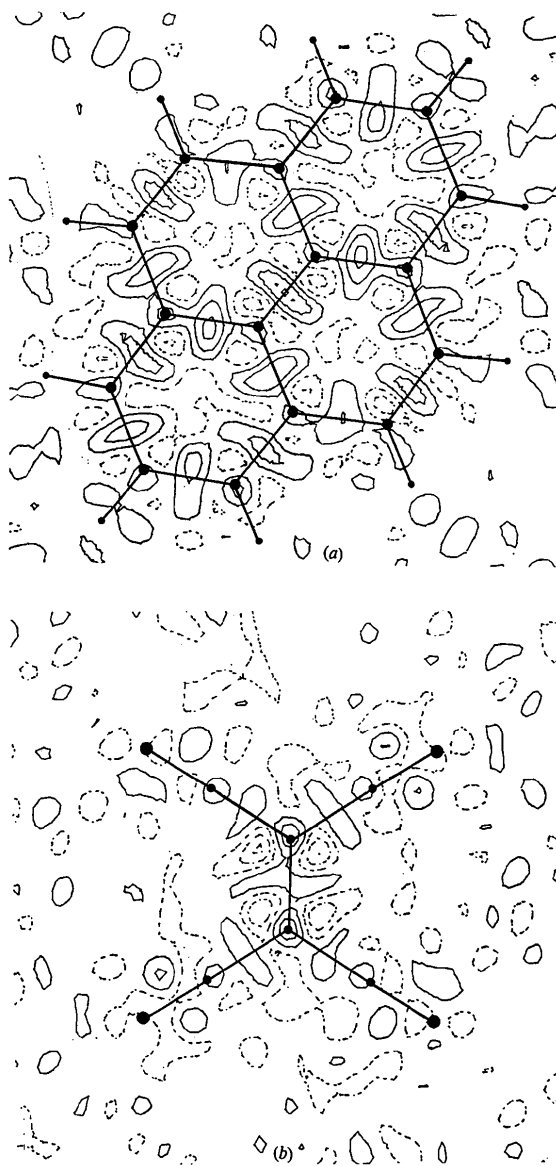

Fig. 2. Difference Fourier density in the plane of the TCNE (a) and the pyrene (b) molecules after disordered model 2 refinement. Contour interval is 0·15 e Å⁻³; negative contours are broken.
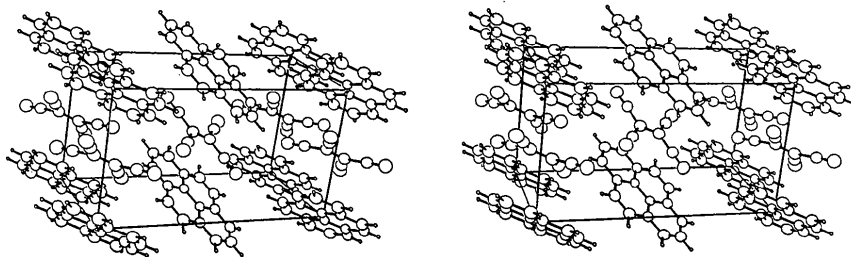

Fig. 3. Molecular packing diagram (stereo pair). The a axis is horizontal in the plane of the paper, while the b axis is pointing away from the viewer.

rotated by 90° ($\varphi_2=\varphi_1+\pi/2$) in the molecular plane around the center of the molecule. TCNE molecules of different occupancy are constrained to identical geometry and identical **T** and **L** tensors.

Table 5. *Observed and calculated structure factors*

H	L	FO	SIG	FC	EX
[illegible]	[illegible]	[illegible]	[illegible]	[illegible]	[illegible]

Table 5 (*cont.*)

H	L	FO	SIG	FC	EX
[illegible]	[illegible]	[illegible]	[illegible]	[illegible]	[illegible]

In another model (3) all Eulerian angles of both types of TCNE molecules are refined independently. The resulting Eulerian angles show differences $\varphi_2-\varphi_1=1\cdot609\simeq\pi/2$, $\theta_2-\theta_1=-0\cdot012\simeq0\cdot0$, and $\Psi_2-\Psi_1=0\cdot046\simeq0\cdot0$, confirming the proposed disordered arrangement

of the TCNE molecules. The R values for the disordered constrained models are significantly better than for the ordered refinement (Hamilton, 1964). Furthermore, the values of the TCNE occupancy factors differ little for the different disordered models, so we conclude that for perdeuteropyrene–TCNE at 105 K 7% of the TCNE molecules are rotated by 90° around the center of the molecule in the molecular plane. Difference maps corresponding to model 2 through the plane of the pyrene molecule (Fig. 2a) and the plane of the TCNE molecule (Fig. 2b) show no significant peaks outside bonding regions. Observed structure factors and the calculated values according to model 2 are listed in Table 5. Final positional parameters and temperature factors from this refinement are listed in Table 2 and Table 3, respectively.

Crystal and molecular structure

The molecular packing of the structure of perdeutero-pyrene–TCNE is shown in Fig. 3. The less populated atomic positions of the disordered TCNE molecule are omitted from the drawing. As found in the earlier structure determination, the most striking feature of the packing arrangement is the alternate stacking of pyrene and TCNE molecules. Intermolecular distances are listed in Table 6. The angle between the normals to the least-squares plane through the carbon atoms of pyrene and the least-squares plane of the TCNE molecule is 2·1°.

Table 6. *Close approaches between molecules*

N···D distances less than 3·1 Å (except for comparison purposes in the column labeled minor TCNE), C···N and C···C less than 3·4 Å. e.s.d.'s: 0·003 Å for C···C; 0·02 Å for N···D. Atoms in the less populated TCNE molecule are primed.

Symmetry code

I	$-x$, $-1-y$, $1-z$;	IV	$\frac{1}{2}-x$, $-\frac{1}{2}+y$, $1-z$
II	$-x$, $-y$, $-z$;	V	$\frac{1}{2}+x$, $-\frac{1}{2}-y$, z
III	$-x$, $-y$, $1-z$;	VI	x, $-1+y$, $1+z$

Between stacks of molecules

Major TCNE		Minor TCNE	
N(1)·····D(6ᴵ)	3·01 Å	N′(2ᴵᴵᴵ)···D(6ᴵ)	3·28 Å
N(1)·····D(8ⱽᴵ)	2·81	N′(2ᴵᴵᴵ)···D(8ⱽᴵ)	2·99
N(1)·····D(2ᴵⱽ)	3·02	N′(2ᴵᴵᴵ)···D(2ᴵⱽ)	3·05
N(1)·····D(7ᴵⱽ)	2·77	N′(2ᴵᴵᴵ)···D(7ᴵⱽ)	2·63
N(2ᴵᴵᴵ)····D(1ᴵ)	2·74	N′(1)·····D(1ᴵ)	2·91
N(2ᴵᴵᴵ)····D(2ⱽ)	2·80	N′(1)·····D(2ⱽ)	2·65
N(2ᴵᴵᴵ)····D(1ⱽ)	2·96	N′(1)·····D(1ⱽ)	2·70
N(2ᴵᴵᴵ)····D(6ᴵ)	2·90	N′(1)·····D(6ᴵ)	3·17

In stack

C(9)······C(1)	3·287 Å	C′(9)·····C(1)	3·305 Å
C(9)······C(2)	3·255	C′(9)·····C(6)	3·245
C(10)·····C(1)	3·203	C′(10)····C(6)	3·296
C(11)·····C(2)	3·248	C′(11)····C(1)	3·208
C(11)·····C(3)	3·382	C′(9ᴵᴵᴵ)···C(3)	3·301
C(9ᴵᴵᴵ)·····C(5)	3·297	C′(10ᴵᴵᴵ)··C(2)	3·299
C(10ᴵᴵᴵ)····C(4)	3·267	C′(10ᴵᴵᴵ)··C(3)	3·321
C(11ᴵᴵᴵ)···C(5)	3·360	C′(11ᴵᴵᴵ)··C(4)	3·260
C(11ᴵᴵᴵ)···C(6)	3·345	N′(2ᴵᴵᴵ)···C(4ᴵᴵ)	3·298
N(1ᴵᴵᴵᴵ)····C(4ᴵᴵ)	3·290		

The disordered arrangement of the TCNE molecules indicates that the interaction between the molecules in

the stacks is not very sensitive to a 90° rotation of TCNE in its molecular plane. The relative population of the two observed positions corresponds to an energy difference ΔE of about 0·54 kcal mole⁻¹, if equilibrium is established at the data-collection temperature. This value must be considered a lower limit. For example if the equilibrium is established during crystallization ($T = 293$ K), and not altered on cooling the energy difference is calculated as 1·6 kcal. These values are to be compared to a calculated difference of 0·27 kcal mole⁻¹ between two relative orientations in the isolated TCNE complex (Herndon & Feuer, 1968). However, it should be noted that neither of the two minima of this calculation corresponds to the experimental geometry in the crystal. Apart from possible differences between the solid state and the isolated complex, there is some doubt that calculations in which the interplanar distance is fixed at an arbitrary value (3·20 Å) have predictive value. In addition interactions between molecules in adjacent stacks may contribute to the energy difference. The two arrangements observed in the crystal structure are approximately related by a local mirror plane passing through C(1), C(4), C″(4) and C″(1) (Fig. 4), which explains the small size of the energy difference. In the paracyclophane–TCNE complex, in which this type of disorder was first observed (Bernstein & Trueblood, 1971), ΔE is 0·7 kcal mole
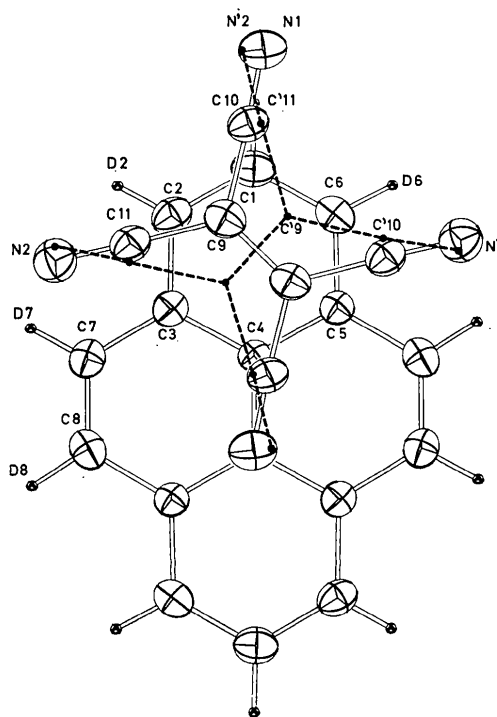

Fig. 4. View of the complex in a direction normal to the least-squares plane of the pyrene molecule showing the two positions of the TCNE molecules relative to the adjacent pyrene molecule. The TCNE molecule depicted with dashed lines represents 7% occupancy. Deuterium atoms have been given an arbitrary radius, other atoms are indicated by their 50% probability ellipsoids.

at room temperature. The arrangement of the pyrene molecules around the TCNE molecule is further illustrated in Fig. 5.

In what follows the geometry of the constituent molecules of perdeuteropyrene–TCNE is described and compared with the geometries of these molecules in different crystal structures (Tables 7 and 8). The numbering of the atoms and the lettering of the bonds are shown in Fig. 6, which also shows bond lengths and angles in the molecules as determined with model 2.

Pyrene

Several experimental and one theoretical set of bond lengths in the pyrene molecule are compared in Table 7.

The lengthening of the C(7)–C(8) (*f*) bond length to 1·42 Å reported by Ikemoto & Kuroda (1968) has not been confirmed, on the contrary the bond lengths of perdeuteropyrene–TCNE are very close to the experimental X-ray and neutron values for molecular pyrene as well as to the mean values of the theoretical calculations.

We note that on the average the peripheral C–C bond lengths in molecular pyrene as determined by X-rays (column 6) are shorter than those determined by neutron diffraction (column 4). This corresponds to a small displacement of the centroids of the atomic charge clouds towards the center of the molecule, which

can be explained by overlap density population being larger in the C–C than in the C–H bonds (Hazell, Larsen & Lehmann, 1972). The agreement between the X-ray and neutron values for the central C–C bond [(*e*), 1·430 (2) and 1·429 (4) Å respectively] supports this explanation. Similar discrepancies have been noted for *p*-terphenyl (Rietveld, Maslen & Clews, 1970) and phenanthrene (Kay, Okaya & Cox, 1971).

Differences in bond lengths between the X-ray determinations of pyrene and perdeuteropyrene–TCNE are very small; the effect of complexing on molecular geometry seems to be at most a few thousands of an ångström. The deviations from the least-squares best plane through the carbon atoms in the pyrene molecule are given in Table 9.

Tetracyanoethylene

Table 8 gives a comparison of TCNE geometries observed in different compounds and with different techniques. The constrained refinement of the disordered model (2) showed an increase in the central C=C bond length of 0·010 Å and in the C≡N bond length of about 0·007 Å and a decrease of the C–C bond length of about 0·006 Å, when compared with the refinement of the ordered model (1). The dimensions given by the disorder model are considered to be more reliable, but not accurate enough to warrant a correc-

Table 7. *Dimensions in the pyrene molecule averaged over chemically equivalent bonds*

	1	2	3	4	5	6	7	8	9
a	1·388 (3)	1·390 (3)	1·391 (3)	1·395 (2)	1·394	1·379 (3)	1·394 (3)	1·403 (6)	1·388 (14)
b	1·400 (3)	1·400 (3)	1·401 (3)	1·406 (2)	1·401	1·405 (4)	1·390 (3)	1·394 (5)	1·406 (12)
c	1·420 (2)	1·421 (2)	1·423 (2)	1·425 (2)	1·415	1·424 (3)	1·417 (3)	1·430 (2)	1·419 (11)
d	1·437 (3)	1·439 (3)	1·440 (3)	1·438 (2)	1·445	1·434 (3)	1·437 (4)	1·445 (3)	1·429 (13)
e	1·427 (3)	1·422 (3)	1·423 (3)	1·430 (2)	1·428	1·429 (4)	1·418 (4)	1·426 (1)	1·445 (11)
f	1·350 (3)	1·351 (3)	1·352 (3)	1·367 (3)	1·361	1·341 (4)	1·346 (5)	1·352 (2)	1·421 (13)

1. Pyrene–TCNE, present work, ordered model. 2. Pyrene–TCNE, present work, disorder of TCNE moiety. 3. Pyrene–TCNE, present work, disorder model, corrected for rigid-body thermal motion. 4. Pyrene, Hazell, Larsen & Lehmann (1972). Neutron determination of molecular pyrene. 5. Mean bond lengths of theoretical calculations on pyrene from a compilation by Hazell, Larsen & Lehmann (1972). 6. Pyrene, Allmann (1970). X-ray determination of molecular pyrene. 7. 2,7-Di-t-butylpyrene, Hazell & Lomborg (1972). 8. Pyrene–pyromellitic dianhydride, Herbstein & Snyman (1969). X-ray data at 110 K. 9. Pyrene–TCNE, Ikemoto & Kuroda (1968).

Table 8. *Dimensions in the TCNE molecule*

	1	2	3	4	5	6	7	8	9
C=C	1·342 (4)	1·352 (4)	1·355 (2)	1·344 (3)	1·357 (10)	1·339 (8)	1·351 (14)	1·348 (7)	1·309 (12)
C–C	1·452 (3)	1·445 (3)	1·431 (1)	1·439 (2)	1·435 (10)	1·441 (5)	1·426 (7)	1·469 (5)	1·472 (13)
	1·450 (3)					1·442 (5)		1·469 (5)	1·464 (12)
C≡N	1·134 (2)	1·143 (2)	1·160 (1)	1·153 (2)	1·162 (2)	1·133 (5)	1·131 (8)	1·136 (10)	1·113 (12)
	1·137 (2)					1·135 (6)		1·147 (10)	1·124 (12)
C=C–C	120·6 (2)	121·1 (2)	122·0 (1)	122·2 (1)	121·1	121·0 (4)	120·9 (3)	119·2 (4)	120·3 (9)
	121·0 (2)					120·9 (4)		119·3 (3)	121·4 (9)
C–C–C	118·4 (2)	117·8 (2)	116·1 (1)	115·6 (2)		118·1 (3)	118·3 (6)	121·4 (4)	118·3 (7)
C–C≡N	177·4 (2)	179·6 (2)	177·9 (1)	178·2 (2)		179·1 (4)	178·7 (8)	173·1 (5)	176·7 (9)
	178·2 (2)					179·4 (4)		174·4 (7)	177·4 (9)

1. Pyrene–TCNE, present work, ordered model. 2. Pyrene–TCNE, present work, disorder of TCNE moiety, model 2. 3. Cubic TCNE, Becker, Coppens & Ross (1973). Neutron diffraction study. 4. Cubic TCNE, Little, Pautler & Coppens (1971). X-ray diffraction study. Distances corrected for riding motion. 5. Gas phase TCNE, Hope (1968). Electron diffraction determination. 6. Monoclinic TCNE, Bekoe & Trueblood (1964). C–C corrected for thermal motion. 7. Naphthalene–TCNE, Williams & Wallwork (1967). 8. [3,3]Paracyclophane–TCNE, Bernstein & Trueblood (1971). Bond lengths corrected for libration by method of Busing & Levy (1964). 9. Pyrene–TCNE, Ikemoto & Kuroda (1968).

Table 9. *Deviations* $(\text{Å} \times 10^3)$ *from the least-squares best plane through the carbon framework in the pyrene molecule*

(Disordered model; TCNE molecule constrained to be planar)

C(1)	+9	C(5)	−4
C(2)	−11	C(6)	+5
C(3)	+1	C(7)	−1
C(4)	−4	C(8)	+7

tion for thermal motion. Compared with the cubic modification of TCNE the C–C bond length is somewhat longer and the C≡N bond length is somewhat shorter in the complex, but a discussion of these differences involving a partially disordered structure seems unwarranted.

Net atomic and molecular charges

The charge on a molecule in a complex can be obtained by integration of the density over the molecular volume. Such an integration was performed, with photographic data, for the triclinic modification of the benzo-

quinone–hydroquinone charge-transfer complex (Sakurai, 1965). A transfer of 0·21 e to the electron acceptor (in this case benzoquinone) was obtained.

A similar calculation for the monoclinic modification of the complex produced a larger value of 0·71 e for the charge transfer to the electron acceptor (Sakurai, 1968). In the present work the integration was performed by means of a general analytical expression (Coppens & Hamilton, 1968), which allows variation of the box-shaped integration volume. Since the TCNE molecule is approximately square, the two box dimensions parallel to the molecular plane (parallel and perpendicular to the central C=C bond) were taken to be equal. An initial value of 3·3 Å was selected for the thickness of the molecule, and the integrated density was plotted as a function of the in-plane dimension. The resulting curve (Fig. 7a) shows an inflexion point at about 6·8 Å, indicating that for this box dimension the best separation between TCNE and neighbouring molecules is obtained. Using this value for the in-plane dimension, the box thickness was varied. This curve (Fig. 7b) has an essentially horizontal section around 3·2 Å, in good agreement with the mean value of 3·4 Å
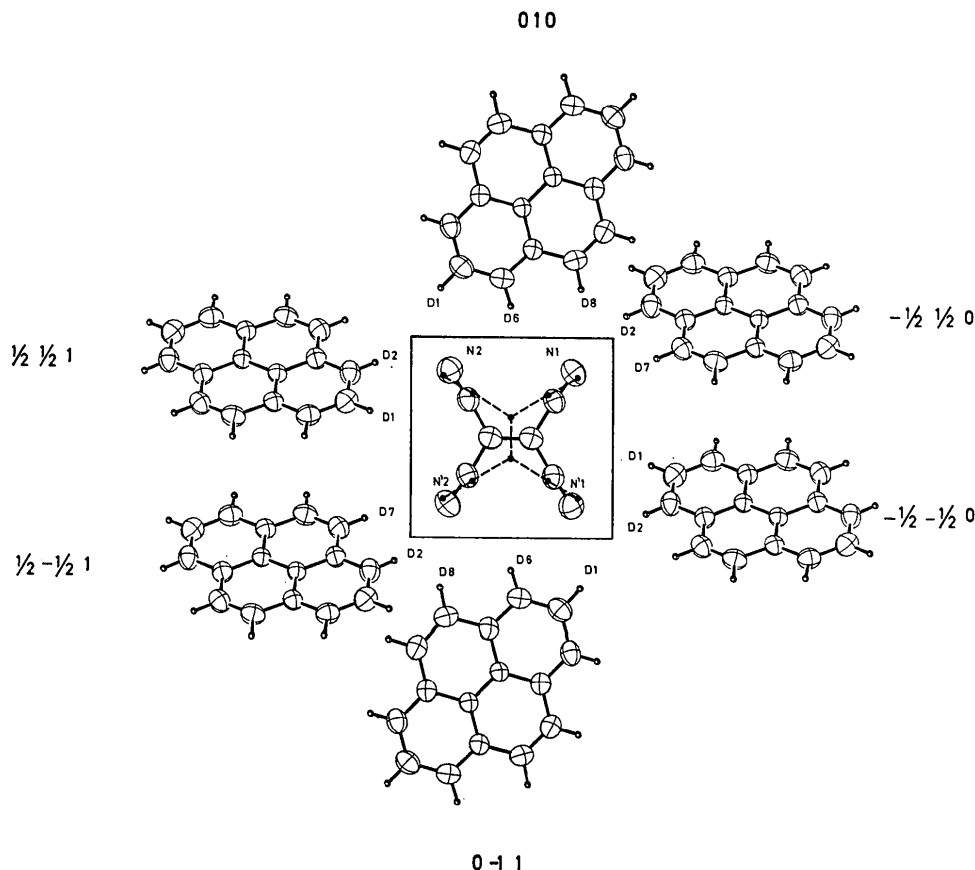

Fig. 5. Packing of pyrene molecules around the TCNE molecule at $00\frac{1}{2}$ viewed normal to the plane of the TCNE molecule. The triplet of numbers beside each pyrene molecule denotes the center of that molecule in terms of unit-cell translations. The square outlines the box over which the electron density of the TCNE molecule was integrated.
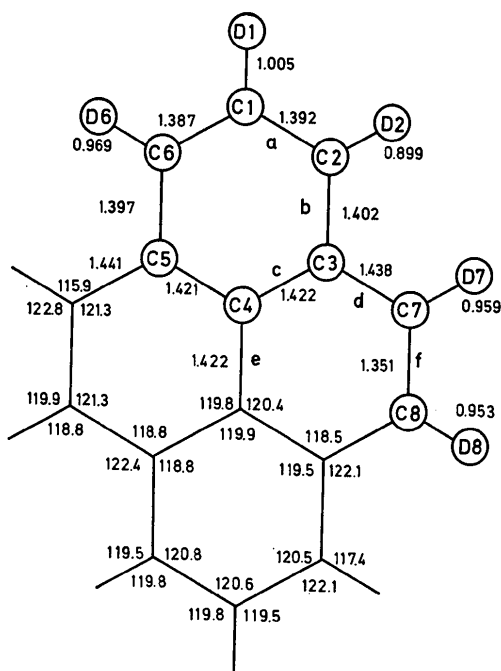
Fig. 6. Bond lengths and angles of the pyrene molecule according to the disordered model 2 refinement, and labeling of atoms and bonds.
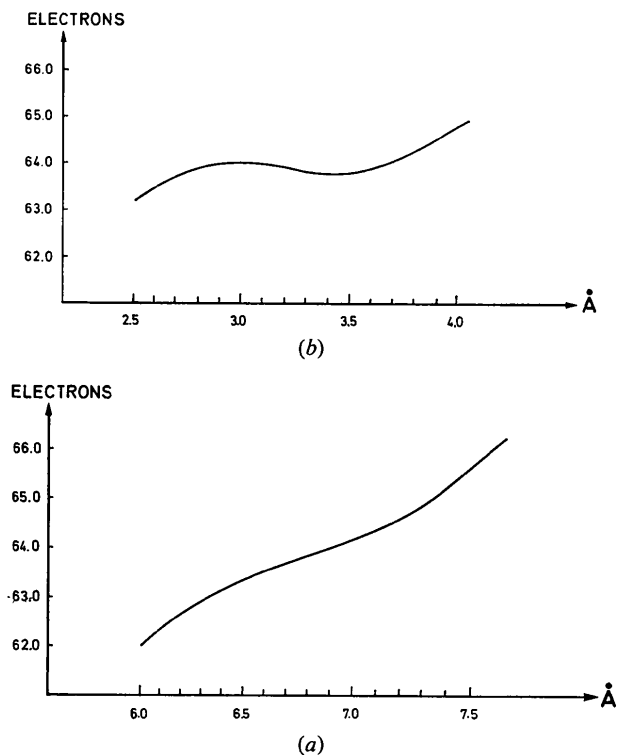

(b)

(a)

Fig. 7. Integrated electron density around the TCNE molecule. Box-shaped integration volume varied for constant thickness of 3·3 Å, number of electrons as a function of dimension of square box (a) and for constant in-plane dimensions 6·8 × 6·8 Å², number of electrons as a function of box thickness (b).

for close approaches between atoms in the stacks of pyrene and TCNE molecules. The horizontal section corresponds to a charge transfer of −0·03 to +0·25 e, the TCNE molecule being slightly positive. It is of interest that the total number of electrons in the box (63·89) is close to the value obtained if only $F(000)$ had been considered (63·14 e for a 6·8 × 6·8 × 3·2 Å box). The average density in the box is therefore close to the average electron density in the crystal, as may be expected in a molecular crystal containing only light atoms. This implies that only the difference between the two values is sensitive to changes in the least-squares scale factor used to put the observations on an absolute scale. Thus, a change of 5% in the scale factor would alter the charge transfer by 0·05 × (63·89−63·14) which is about 0·04 e.

The box over which integration was performed, and its relation to neighbouring molecules is shown in Fig. 5.

Values for the net atomic charges in a number of molecules have been obtained from X-ray diffraction data using an L-shell projection method (Stewart, 1970; Coppens, Pautler & Griffin, 1971). In oxalic acid dihydrate, cyanuric acid and the Ni diethylenediamine malonate complex, charges were obtained which agreed fairly well with a Mulliken population analysis of semi-empirical INDO (intermediate neglect of differential overlap) calculations (Coppens et al., 1971). Similarly, in the light-atom mineral kernite ($Na_2B_4O_7.4H_2O$) the charges correlated quite well with atomic electronegativity (Cooper, Larsen, Coppens & Giese, 1973). In tetracyanoethylene (Little, Pautler & Coppens, 1971) and in tetracyanoethylene oxide (Matthews, Stucky & Coppens, 1972) on the other hand, the charges for the cyano group atoms were small and not in agreement with other evidence which supports the strongly dipolar nature of this group.

In the charge refinement of the low-temperature data of the perdeuteropyrene–TCNE complex with the ELS (Extended L-Shell projection) method, the charges on

Table 10. Net charges from extended L-shell projection (ELS) refinement (STO basis set)

Owing to rounding-off of the table entries, the sum of the charges in TCNE–pyrene is slightly different from zero. The net charges on the TCNE and pyrene molecules from this refinement are respectively +0·07 and −0·07 units.

C(1)	−0·04 (4)	C(8)	+0·03 (4)
C(2)	+0·05 (4)	H(1)	+0·05 (3)
C(3)	−0·19 (4)	H(2)	+0·02 (3)
C(4)	−0·02 (3)	H(6)	+0·02 (3)
C(5)	−0·17 (4)	H(7)	+0·04 (3)
C(6)	+0·14 (5)	H(8)	+0·03 (3)
C(7)	+0·03 (4)		

	TCNE in TCNE–pyrene	TCNE in cubic tetracyanoethylene	TCNE in TCNE–perylene
C(9)	+0·11 (3)	+0·20 (2)	+0·11 (5)
C(10)	−0·01 (4)	−0·09 (3)	+0·04 (3)
C(11)	+0·06 (4)		+0·04 (5)
N(1)	−0·01 (3)	−0·01 (3)	−0·04 (5)
N(2)	−0·12 (3)		−0·02 (5)

the disordered TCNE molecule were constrained to be equal to the charges on the molecules in the site with 93·0% occupancy. Furthermore, the geometry and thermal motion of the disordered molecule were not varied, which seemed justified as the shifts in atomic parameters during the ELS refinement were very small.

The resulting charges (with STO basis functions) (Stewart, 1970) are listed in Table 10. The values for the individual atoms are small and rather similar to corresponding values on the TCNE molecules in cubic TCNE and TCNE–perylene (Coppens, Pautler & Griffin, 1971). When summed over each of the molecules of the complex, the refinement leads to a charge transfer of 0·07 e from the TCNE molecule in reasonable agreement with the value of +0·11 units of charge at the midpoint of the horizontal section of the curve in Fig. 7. The direction of the apparent transfer is opposite to what would be expected from the molecular electronegativities (Foster, 1969, p. 387), but the effect is small and probably not significantly different from zero. Thus, it appears from the diffraction results that the molecules in the ground state of the perdeutero-pyrene–TCNE complex are essentially neutral and that the charge transfer in the ground state is less than 0·15 e per molecule.

References

ADMAN, E., ROSENBLUM, M., SULLIVAN, S. & MARGULIS, T. N. (1967). *J. Amer. Chem. Soc.* **89**, 4540–4542.

ALLMANN, R. (1970). *Z. Kristallogr.* **132**, 129–151.

BECKER, P., COPPENS, P. & ROSS, F. K. (1973). *J. Amer. Chem. Soc.* **95**, 7604–7609.

BEKOE, D. A. & TRUEBLOOD, K. N. (1960). *Z. Kristallogr.* **113**, 1–22.

BEKOE, D. A. & TRUEBLOOD, K. N. (1964). Abstract A.C.A. Meeting. Bozeman, Montana p. 87. Final report AFOSR-240-63.

BERNSTEIN, J. & TRUEBLOOD, K. N. (1971). *Acta Cryst.* B**27**, 2078–2089.

BUSING, W. R. & LEVY, H. A. (1964). *Acta Cryst.* **17**, 142–146.

BUSING, W. R. & LEVY, H. A. (1967). *Acta Cryst.* **22**, 457–464.

COOPER, W. F., LARSEN, F. K., COPPENS, P. & GIESE, R. F. (1973). *Amer. Min.* **58**, 21–31.

COPPENS, P. & HAMILTON, W. C. (1968). *Acta Cryst.* B**24**, 925–929.

COPPENS, P., PAUTLER, D. & GRIFFIN, J. F. (1971). *J. Amer. Chem. Soc.* **93**, 1051–1058.

COPPENS, P., ROSS, F. K., BLESSING, R. H., COOPER, W. F., LARSEN, F. K., LEIPOLDT, J. G., REES, B. & LEONARD, R. (1974). *J. Appl. Cryst.* **7**, 315–319.

COULTER, C. L. (1960). Doctoral dissertation, Univ. of California, L. A.

FOSTER, R. (1969). *Organic Charge-Transfer Complexes.* London and New York: Academic Press.

HAMILTON, W. C. (1964). *Statistics in Physical Science.* New York: Ronald Press.

HAZELL, A. C., LARSEN, F. K. & LEHMANN, M. S. (1972). *Acta Cryst.* B**28**, 2977–2984.

HAZELL, A. C. & LOMBORG, J. G. (1972). *Acta Cryst.* B**28**, 1059–1064.

HERBSTEIN, F. H. & SNYMAN, J. A. (1969). *Phil. Trans. Roy. Soc.* A**264**, 635–645.

HERNDON, W. C. & FEUER, J. (1968). *J. Amer. Chem. Soc.* **90**, 5914–5915.

HOPE, H. (1968). *Acta Chem. Scand.* **22**, 1057–1058.

IKEMOTO, I. & KURODA, H. (1968). *Acta Cryst.* B**24**, 383–387.

IKEMOTO, I., YAKUSHI, K. & KURODA, H. (1970). *Acta Cryst.* B**26**, 800–806.

KAY, M., I., OKAYA, Y. & COX, D. E. (1971). *Acta Cryst.* B**27**, 26.

LITTLE, R. G., PAUTLER, D. & COPPENS, P. (1971). *Acta Cryst.* B**27**, 1493–1499.

MATTHEWS, D. A., STUCKY, G. D. & COPPENS, P. (1972.) *J. Amer. Chem. Soc.* **94**, 8001–8008.

PAWLEY, G. S. (1971). *Advances in Structure Research by Diffraction Methods*, Vol. 4, edited by W. HOPPE & R. MASON. Oxford: Pergamon Press.

RIETVELD, H. M., MASLEN, E. N. & CLEWS, C. J. B. (1970). *Acta Cryst.* B**26**, 693.

SAKURAI, T. (1965). *Acta Cryst.* **19**, 320–330.

SAKURAI, T. (1968). *Acta Cryst.* B**24**, 403–412.

SCHOMAKER, V. & TRUEBLOOD, K. N. (1968). *Acta Cryst.* B**24**, 63–76.

STEWART, R. F. (1970). *J. Chem. Phys.* **53**, 205–213.

WILLIAMS, R. M. & WALLWORK, S. C. (1967). *Acta Cryst.* **22**, 899–906.